Indian Journal of Fibre & Textile Research
Vol. 50, December 2025, pp. 387-396
DOI: 10.56042/ijftr.v50i4.14032

Incorporation of carbonised water hyacinth for increasing mechanical, thermal, and odour properties of fabrics

Toufique Ahmed[1,a], A Al Adriar[2], Md Monir Hossain[2], Rubayeath Jahan Raka[2], Md Oarka Bin Seraz[2], Jannatul Nayeem Shiham[2] & Tanzeena Refat Tumpa[2]

[1]Department of Textile Engineering, Faculty of Engineering, Daffodil International University, Dhaka 1216, Bangladesh

[2]Department of Textile Engineering, National Institute of Textile Engineering and Research, Dhaka 1350, Bangladesh

Received 27 September 2024; revised received and accepted 21 May 2025

This study aims to carbonise water hyacinth, activate it chemically using $ZnCl_2$, and apply the resulting material in textile finishing to enhance selected properties of clothing. Water hyacinth, a widely occurring free-floating perennial aquatic weed, is often regarded as invasive; its conversion into a value-added textile finish therefore presents both environmental and functional benefits. The carbonisation process produces concave, oval-shaped carbon nanoparticles measuring approximately 200 nm by 100 nm, which are subsequently applied to fabrics using padding, coating, coat–pad curing, and infrared dyeing techniques. Among these, the coated samples produced through multiple padding cycles exhibit the most promising performance in terms of FTIR characteristics, air permeability, and stiffness. Although the treatment does not significantly improve mechanical properties such as tensile, bursting, or tear strength, it does enhance thermal behaviour, yielding a 13.8% increase in thermal insulation (CLO) and a 14.3% increase in thermal resistance ($m^2 \cdot K/W$). Notably, the treated samples also demonstrate 100% odour resistance. Energy Dispersive Spectroscopy confirms the material composition, showing 99.32% carbon and 0.32% zinc distributed uniformly across the examined areas, indicating successful particle deposition.

Keywords: Activated carbon, Carbonisation, Carbon nanoparticles, Odour resistance, Thermal resistance, Water hyacinth

1 Introduction

Carbon plays a crucial role in numerous industrial applications, particularly in the petrochemical sector, where carbon-based materials are used to manufacture plastics, paints, fibres, polymers, and solvents. In metal smelting, impure forms of carbon—such as coke derived from coal and charcoal produced from wood—serve as essential reducing agents. Activated carbon, a processed form of carbon with enhanced porosity and a high surface area, is widely employed as an adsorbent due to its exceptional capacity to capture impurities and pollutants[1]. For instance, activated carbon is capable of removing volatile organic compounds such as toluene from enclosed area[2]. Owing to its porous structure, it finds extensive application in hydrogen and methane storage, air and water purification, supercapacitors, solvent recovery, gold extraction, decaffeination, medicine, sewage treatment, respirator filters, compressed air filtration, teeth whitening, and agricultural processes[3,4]. Its cost-effectiveness and versatility have further enabled its use in batch and fixed-bed adsorption systems for environmental remediation[5], while sewage sludge (SS)-based activated carbon (SBAC) has recently emerged as an eco-friendly option for removing phenolic compounds from wastewater[6].

Carbonisation, the process of converting biomass into carbon-rich material, typically involves pyrolysis—heating organic matter within a controlled temperature range. Low-temperature carbonisation occurs between 300–400 °C, whereas high-temperature carbonisation takes place between 400–800 °C. Hydrothermal carbonisation, another environmentally friendly method, converts wet biomass, agricultural waste, and municipal waste into hydrochar using hot, compressed water under subcritical conditions; the resulting hydrochar is often used as a soil enhancer. A variety of plant sources, including bamboo, pineapple roots, and the stems and roots of *Mahonia oiwakensis*, have been employed to produce carbon nanodots (CNDs) through carbonisation[7].

Water hyacinth (*Eichhornia crassness*) is a highly invasive aquatic plant that significantly disrupts freshwater ecosystems by altering floral diversity and forming dense biomass mats. These mats impede

[a]Corresponding author.
E-mail: atoufique@gmail.com

navigation, fishing, and water transport, and frequently clog waterways[8]. Despite these challenges, water hyacinth contains appreciable amounts of cellulose, hemicellulose, and lignin, making it a promising raw material for biomass utilisation. According to Lahon *et al*.[9], water hyacinth can yield as much as 408.1 tonnes of biomass per hectare in peak growing seasons.

Extensive research highlights the plant's potential in sustainable resource applications. It can be used for biogas production[10], biomethane recovery[11] and soil improvement[12]. More recently, it has been explored as a precursor for activated carbon via pyrolysis because of its excellent adsorptive characteristics and well-developed micro- and mesoporous structure[13]. This expanding utilisation also contributes to ecological restoration by removing excess biomass from affected water systems.

Several studies have incorporated water hyacinth–derived activated carbon into textile materials to improve fabric performance. Activated carbon's high surface area allows it to adsorb odour-causing compounds generated by microbial degradation of sweat. Similarly, neem-charcoal-treated fabrics have shown enhanced wetting, wicking, and water vapour permeability properties[14]. Water hyacinth–based activated carbon (WHAC) typically exhibits a high specific surface area (912–1,066 m^2/g) and contributes to excellent thermal insulation[5]. Moreover, blending water hyacinth fibres with hemp has been shown to increase the thermal resistivity of nonwoven fabrics by reducing thermal conductivity.

Body odour in textiles primarily results from the interaction between sweat and microorganisms, especially the gram-positive bacteria, that metabolise sweat components and release volatile pungent odour[15,16]. Although sweat itself is initially odourless, fabrics, particularly cotton, provide a favourable environment for bacterial proliferation, leading to odour formation, discolouration, and fabric degradation[17]. Body odour becomes more prominent after puberty, originating mainly from the axillary region and subsequently transferring to clothing. The odour profile of textiles differs from that of the skin due to environmental conditions such as humidity, airflow, and the presence of antimicrobial agents[18]. Antibacterial finishes, therefore, play a vital role in mitigating odour by limiting microbial growth.

Given the increasing demand for sustainable, functional textile treatments, this study aims to evaluate the potential of carbonised and chemically activated water hyacinth as a textile finish. The work investigates its effectiveness in improving selected mechanical properties, enhancing thermal resistance, and imparting odour-control functionality when applied to fabrics.

2 Materials and Methods

2.1 Materials

Water hyacinth plants, cotton knit fabrics, woven cotton fabrics, hydrochloric acid (HCl), and zinc chloride ($ZnCl_2$) were used in this study. Water hyacinth was collected from a local river in September, while the knit and woven fabrics were sourced from a local textile factory. For preparing the finishing paste, sodium carbonate (Na_2CO_3), thickener, urea (a hygroscopic agent), sequestering agent, levelling agent, binder, and Glauber's salt (sodium sulphate) were used. All chemicals were of analytical grade and were used without further purification.

2.2 Machinery

A pad–dry–cure machine, an infrared (IR) dyeing machine, a muffle furnace, and a magnetic stirrer were used for sample preparation. Air permeability is measured using the TEXTEST FX-3300 instrument, which determines the ease with which air passes through fabrics. The tensile strength of woven fabrics is evaluated using the Digi-Strength tester by Paramount, while tear strength is measured with the Elmendorf Tear Tester (model 455/02/1123) from James H-Heal. The bursting strength of knitted fabrics is assessed using the MESDAN-Lab tester (model 338 E). Thermal properties are measured with the TESTEX TF130 instrument. For structural and chemical characterisation, a PerkinElmer Spectrum Two Fourier Transform Infrared Spectrometer (FTIR) and a Zeiss Field Emission Scanning Electron Microscope (FESEM) are used, along with the corresponding Energy Dispersive X-ray Spectroscopy (EDS) system to determine elemental composition.

2.3 Methods

The entire method is depicted in Fig. 1. First, water hyacinth plants were collected, cleaned, and the leaves were removed. The material was washed, dried, chopped and boiled in 0.25 M HCl. After rinsing and freeze-drying, the biomass was crushed, ground and sieved to obtain particles in the range of 1.4–2.0 mm. 40 g of these dried particles were added to a zinc chloride ($ZnCl_2$, ≥98 %) solution and stirred

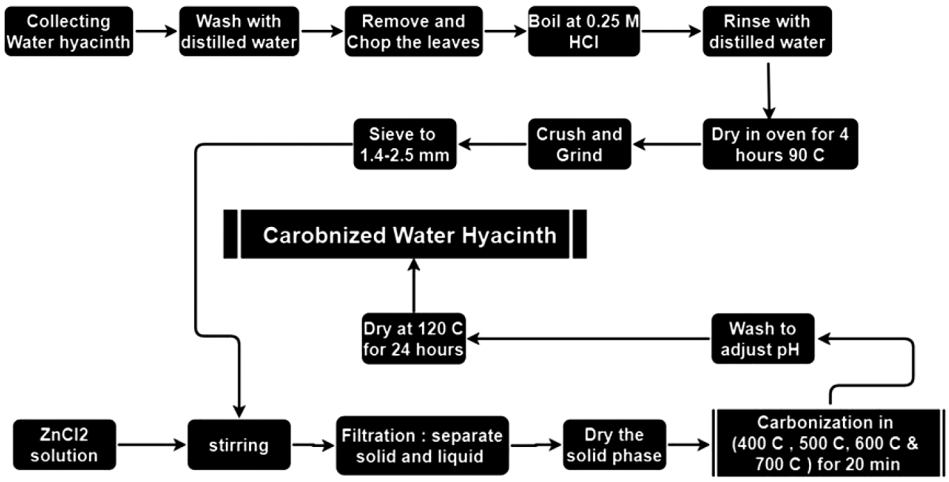

Fig. 1 — Schematic presentation of the process used for carbonising water hyacinth

at 60 °C for 4 h for chemical activation. The mixture was filtered, and the solid fraction was dried at 105 °C for 24 h. Carbonisation was carried out in an electric furnace at 400, 500, 600 and 700 °C for 20 min each. After carbonisation, the particles were rinsed with 0.5 M HCl to remove $ZnCl_2$, followed by repeated washing with hot distilled water until a neutral pH was achieved. The resulting product was dried at 110 °C for 12 h and stored in labelled containers.

2.3.1 Carbonisation Process of Water Hyacinth

Water hyacinth leaves were chopped and shade-dried for seven days. To remove metallic oxides, the dried leaves were boiled in 0.25 M HCl and thoroughly rinsed with distilled water. The leaves were oven-dried at 90 °C for 4 h, ground and sieved. In the next stage, 40 g of the sieved leaves were mixed with 98 % zinc chloride ($ZnCl_2$) and stirred at 60 °C for 4 h for chemical activation. The solid and liquid phases were separated by filtration, and the solid material was dried at 105 °C for 24 h.

Carbonisation was done in an electric furnace at 400, 500, 600, and 700 °C for 80 min at each temperature step. The resulting activated carbon was rinsed with 0.5 M HCl to remove $ZnCl_2$ and subsequently washed with hot distilled water until a neutral pH was achieved. Finally, the carbonised water hyacinth was dried at 110 °C for 12 h, yielding 15 g of carbonised water hyacinth nanoparticles, which were stored in labelled vessels for future use.

2.3.2 Incorporation into Fabrics

Carbonised water hyacinth particles were applied to woven and knit fabrics using immersion, IR dyeing, coating, and padding methods. A treatment solution was prepared using 3 g/L carbonised water hyacinth, 2 g/L urea (hygroscopic agent), 3 g/L Glauber's salt, 15 g/L binder, and 1 ml/L each of wetting, sequestering, and levelling agents. The material-to-liquor ratio (MLR) was set at 1:10. The paste was applied using various methods, including padding, coating, and IR dyeing. Treatment curves for padding and coating are shown in Fig. 2(a), while the curve for IR dyeing is shown in Fig. 2(b).

Initial coated samples were rigid; therefore, additional padding was performed to improve flexibility. A separate set of samples underwent multiple padding treatments to ensure deeper penetration of particles. The prepared samples are detailed in Table 1.

2.3.2 Thermal Resistance

The thermal test was conducted in accordance with the ISO 11092:2014 standard. Single jersey knit cotton fabric (160 GSM) in white was used, with standard dimensions of 35 × 35 cm. Two samples, one untreated control and one treated with carbonised water hyacinth, were tested. The treated samples were prepared using various chemicals, including activated carbon particles and a binder. The thermal resistance (R_{ct}) was calculated using Eq. 1:

$$R_{ct} = \frac{(T_m - T_a)}{(H - \delta H_c)} \quad \ldots(1)$$

where R_{ct} is thermal resistance of the fabric (m^2K/W); $T_{m,}$ = temperature of the metal plate (K); T_a, temperature of the test area (K); H, heating power of the metal plate (W); δH_c, heating power correction factor; and S, surface of the metal plate (m^2).

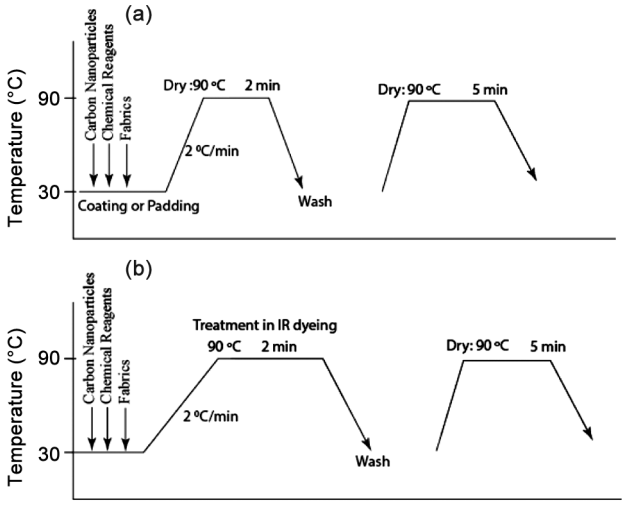

Fig. 2 — Treatment curves of carbonised water hyacinth nanoparticles using (a) padding and coating method, and (b) IR dyeing method

Table 1 — Preparation details of different fabric samples

Sample	Fabric type	Fabric pre-treatment	Loading method
KF control	Knit	Raw sample	NIL
WF control	Woven	Raw sample	NIL
WF pad	Woven	Scouring and bleaching	Padding
KF pad	Knit	Scouring and bleaching	Padding
KF IR	Knit	Scouring and bleaching	IR dyeing
WF coat	Woven	Scouring and bleaching	Coating
KF coat pad	Knit	Scouring and bleaching	Coating and padding
KF coat pad multi	Knit	Scouring and bleaching	Coating and padding multiple times

The test was conducted at a plate temperature of 35°C, with an airflow of 1 ± 0.05 m/s. The apparatus thermal resistance was 0.049 m². k/W.

2.4 Mechanical Tests

2.4.1 Tensile Strength

Tensile strength of woven fabrics was measured according to ASTM D5034 using the Digi-Strength Tester (Paramount, India). Grab test specimens measuring 200 × 100 mm were used, and a force was applied to assess their load-bearing capacity. Results from treated samples were compared with those from untreated (control) samples, and averages were calculated along with standard errors (SE) using Eq. 2.

$$SE = \frac{\sigma}{\sqrt{N}} \quad \ldots(2)$$

where σ is the sample standard deviation; and N, total number of samples.

2.4.2 Tear Strength

It describes a fabric's ability to withstand tearing or rip propagation under the influence of outside forces. The ASTM D624 is the most common method for the tear test. It precisely quantifies the force required to initiate and sustain a rip in the cloth, often in a specific direction. Here, fabric specimens (100 × 75 mm) were subjected to a specified force, and the force required to cause a tear to propagate was recorded.

2.4.3 Bursting Strength

It is the force required to rupture a woven or knitted fabric by dilating it with a force applied perpendicular to the sample's plane under standard conditions. Bursting strength of knit fabrics was assessed according to ASTM D3786 using a Constant Rate of Elongation (CRE) bursting tester. Specimens (90 × 90 mm) were clamped over a rubber diaphragm, and air pressure was applied until the specimens ruptured. Burst pressure was displayed digitally.

2.3 Odour Test

The odour evaluation procedure was adapted from McQueen *et al.*[19] with a key enhancement for clarity. For this study, five male participants aged 22-25 (weighing between 58-80 kg) were carefully selected from the university, and institutional ethical approval was obtained. Participants were informed about the study procedures and confirmed that the treated fabrics contained no harmful substances.

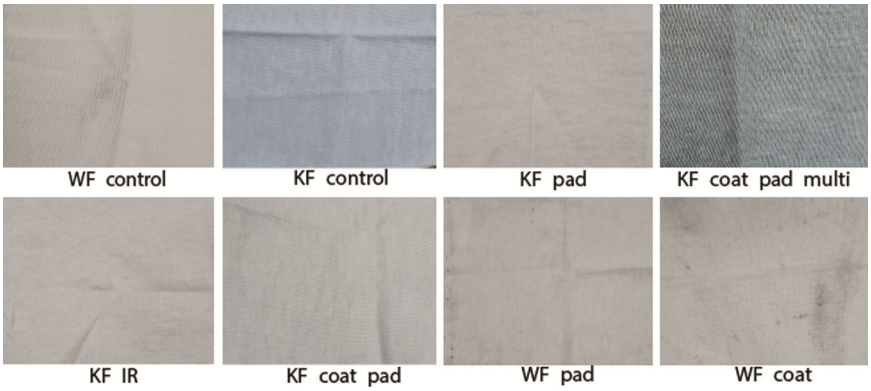

Fig. 3 — Visual appearance of the different treated and untreated samples

To avoid interference, participants were instructed not to use deodorants, perfumes, or antibacterial lotions and to refrain from consuming spicy foods for 48 hours prior to testing. Each participant engaged in over two hours of physical activity to induce sufficient perspiration. All fabric samples were exposed to sweat and subsequently sealed in airtight polybags labelled with sample details.

After one week, odour intensity was assessed by a panel of four evaluators using a five-point scale: very bad (1), bad (2), moderate (3), good (4), and very good (5). The statistical mode was calculated for each sample, and the SE was computed using Eq. 2. This structured approach ensures a reliable, reproducible, and scientifically robust odour assessment.

3 Results and Discussion

The carbonised water hyacinth particles were incorporated into the knit and woven samples by padding, coating, and IR dyeing methods. The visual appearance of the treated samples is shown in Fig. 3.

3.1 FTIR

The FTIR spectrum for the selected samples is illustrated in Fig. 4. This analysis highlights several noteworthy features. The Coated sample displays a weak peak at 1734 cm^{-1}. This peak falls within the spectral range of 1650-2000 cm^{-1}, which typically represents C-H bonding in aromatic compounds, indicating that materials containing the C-H functional group are present in the coating material. Additionally, a medium peak at 1030 cm^{-1} is noted, corresponding to C-N stretching vibrations. This peak indicates the presence of an amine group in the Coated sample. In contrast, the padded, IR-treated, and control (cotton) samples exhibit a strong peak at 1027 cm^{-1}. This peak is associated with C-O stretching vibrations within the spectral range of

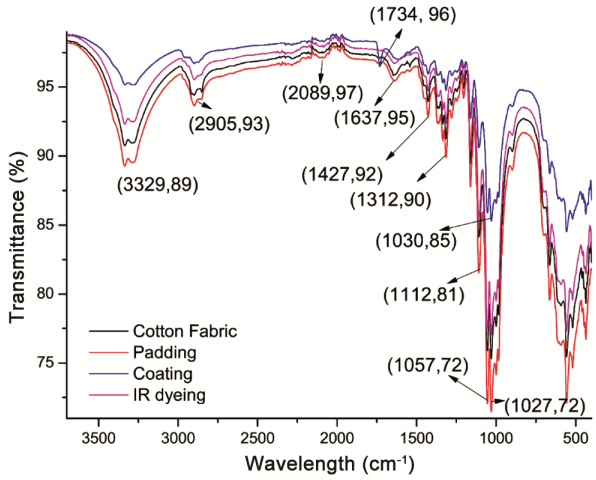

Fig. 4 — FTIR spectra of the various raw and treated samples

1050-1085 cm^{-1}, which is typical of primary alcohols. Among others, the band observed at 3329 cm^{-1} is mainly attributed to the O–H stretching vibration of hydroxyl groups. This strong band suggests the presence of hydroxyl groups that are bonded intermolecularly, indicating potential hydrogen bonding interactions within the structure. Additionally, this band is also associated with the C–H stretching vibration of alkyne compounds, highlighting the coexistence of various functional groups. The band at 2905 cm^{-1} arises from C–H stretching of alkane groups, indicating the presence of saturated hydrocarbons within the material structure. A weaker band at 2086 cm^{-1} is assigned to the N=C=S stretching vibration, characteristic of the isothiocyanate group. This low-intensity band implies that while isothiocyanates are present, they may be in lower abundance compared to other functional groups in the molecule. The band at 1637 cm^{-1} corresponds to aromatic C=C bonds and/or amine groups. This peak suggests the existence of resonance structures

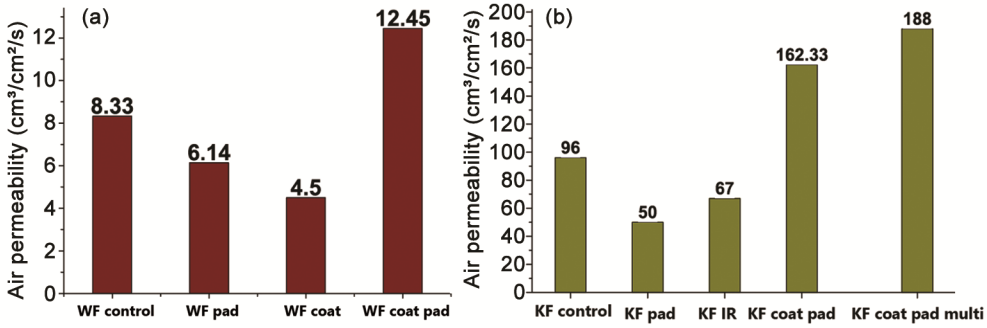

Fig. 5 — Air permeability of different coating treatments applied to (a) woven fabrics, and (b) knitted fabrics

commonly associated with aromatic compounds, which can affect the compound's reactivity and stability. Finally, the sharp band at 1312 cm^{-1} specifically relates to the aromatic amine group, represented by the C–N bond stretching. The clarity of this peak signifies a notable presence of aromatic amines, which may be crucial to the compound's overall properties and interactions. Collectively, the FTIR data provides insight into the diverse functional groups introduced during treatment and their potential influence on fabric behaviour.

3.2 Air Permeability Analysis

The air permeability of various samples made from carbonised water hyacinth, using different loading methods, is shown in Fig. 5 (a). A clear trend is the decrease in air permeability of woven fabrics after treatment with carbonised water hyacinth. The untreated woven fabric exhibits low air permeability (8.33 $cm^3/cm^2/s$). After treatment with the padding method, this value dropped to 6.14 $cm^3/cm^2/s$, indicating a significant loss of breathability. Additionally, using the coating method with carbonised water hyacinth resulted in an even lower air permeability of 6.01 $cm^3/cm^2/s$. Interestingly, when the padding method is combined with the coating, there is a notable increase in air permeability, reaching 12.45 $cm^3/cm^2/s$. This represents a 50 % increase compared to the control woven fabrics. The binder used in coating tends to stiffen the fabric and reduce breathability; therefore, padding is added after coating to restore flexibility and enhance airflow. The low air permeability of woven fabrics is primarily due to their interlaced structure, which restricts airflow. To explore this further, knit fabrics are also assessed [Fig. 5 (b)]. The raw knit fabric shows considerably higher air permeability (96 $cm^3/cm^2/s$) due to its looped structure. Padding reduces air permeability to 50 $cm^3/cm^2/s$. This reduction is likely due to the contraction of the knit loops under the pressure of the padding, followed by the relaxation of the fabric. Similarly, IR dyeing also decreases permeability to 67 $cm^3/cm^2/s$, likely due to the relaxation of fibres during the dyeing process. In contrast, coating followed by padding increases air permeability to 162.33 $cm^3/cm^2/s$—an increase of nearly 70 % compared to the control knit samples. Multiple padding cycles further enhance permeability to 188 $cm^3/cm^2/s$. This marks a remarkable 95 % improvement over the control knit fabrics. These findings indicate that the combination of coating followed by multiple padding is the most effective approach for enhancing air permeability when loading carbonised water hyacinth.

This result can be compared with neem charcoal particles incorporated woven fabrics, which showed 35.38 %, 13.22 %, and 45.07 % decreases for cotton, polyester and P/C blended fabrics, respectively [14].

3.3 Thermal Resistance

Thermal resistance quantifies a fabric's ability to prevent heat transfer[20]. It is essential to prevent energy losses and determine the insulation property of a material[21]. Thermal conductivity refers to a material's capacity to transfer heat and regulate temperature, which ultimately contributes to comfort when wearing clothing. This property is essential in determining how effectively a fabric can insulate or cool the body. Generally, the thermal conductivity of a material is positively correlated with its density; that is, as the density of the fabric increases, its ability to absorb and transmit heat also tends to rise[22]. Material with lower density tends to show superior insulation properties due to entrapped air pockets (thermal conductivity 0.024 W/mK)[20]. For example, mineral wool having 20-200 kg/m^3 has a thermal conductivity within 0.035-0.045 W/mK[23], whereas for stone wool it is 0.036 W/mK (density 32 kg/m^3). Polyurethane insulator, on the other hand, has 0.025 W/mK with 35 kg/m^3 density[24]. The thermal property of clothing is typically expressed in CLO, TOG, or metabolic unit

m² °C/h/Kcal, which can be converted to the standard SI unit m² k/w (1 m² °C/h/Kcal = 0.86 m² k/w). For expressing human heat exchange, another unit named Met (Metabolic Equivalent of Task) is frequently used. It is the quantity of metabolism of a man sitting in a comfortable condition. 1 Met is equivalent to 50 kcal/m^{2}h (i.e., 58.2 W/m^2). Similarly, CLO is used for insulation properties. 1 CLO is the insulation of clothing that is maintained for an average man resting under a comfortable condition (21 °C, 0.1 m/s air velocity, RH 50 %). Normally, human skin can evaporate 24 % of metabolic heat; hence, 0.76 Met (38 kcal/m^{2}h) remains to be lost through radiation, convection, and conduction. Comfortable mean skin temperature is 33 °C. Therefore, total insulation of clothing in ambient air is given by:

$$l_t = \frac{33-21}{38} = 0.32\ m^2\ °C.\,h/Kcal \quad \ldots(3)$$

However, the air insulation is $0.14 m^2 °C.\,h/Kcal$, so the insulation of the clothing is 0.32-0.14 = $0.18 m^2 °C.\,h/Kcal$. Thus, 1 CLO is 0.18 $m^2 °C.\,h/Kcal$ (0.155m2C/W). A warm business suit ensemble provides approximately 1 CLO of insulation for the whole body. TOG is another unit of thermal resistance that can keep the temperature gradient of 0.1℃ with a heat flux of 1 W/m^2. Unlike the CLO, the TOG is a physical measure of thermal resistance and has no direct relevance to human comfort[25]. Light summer suits provide insulation of one Tog. The TOG is a unit of thermal resistance where 1 TOG = 0.1 m^2 K/W[26].

Table 2 presents the thermal properties of the control samples and the treated samples. Here, the carbonised water hyacinth-treated sample shows a 14.3% increase in thermal resistance (from 0.028 to 0.032 m²·K/W) compared with the control. In the TOG unit, it is equivalent to the m^2.k/W unit, since 1 TOG = 0.1 m^2.k/W. Clothing insulation, expressed in CLO, also increases from 0.181 to 0.206 CLO, representing a 13.8% enhancement. These improvements are attributed to the presence of carbonised particles, which create micro air pockets and interrupt heat flow.

Comparable findings in earlier studies demonstrate that water hyacinth-based materials offer improved thermal insulation[27]. Conversely, neem charcoal treatments tend to decrease thermal resistance in cotton, polyester, and P/C blended fabrics by 5.49 %, 16.35 % and 16.88 %, respectively[14]. This suggests that carbon sources and application method strongly influence thermal performance.

3.4 Mechanical Tests Analysis

Fig. 6 (a) presents the results of the tensile, tear, and bursting strength tests conducted on untreated and carbonised water hyacinth-treated fabric samples. The untreated samples show an average tensile strength of 29.74 kg (standard error 0.17), whereas the carbonised water hyacinth-treated samples record a slightly higher value of 30.30 kg (standard error 0.54), reflecting an increase of 0.56 kg. A similar pattern is observed in the tear strength results: the untreated fabrics achieve a strength of 65.53 N (SE 0.08), while the treated samples show a marginally higher strength of 65.87 N (SE 0.06).

In contrast, the bursting strength, measured for knitted samples, decreases following treatment. The

Table 2 — Thermal properties of raw and treated samples

Sample	Thickness	Thermal resistance		
KF control	0.43 mm	0.028 m^2.k/w	0.181 CLO	0.28 TOG
KF coat pad multi	0.47 mm	0.032 m^2.k/w	0.206 CLO	0.32 TOG

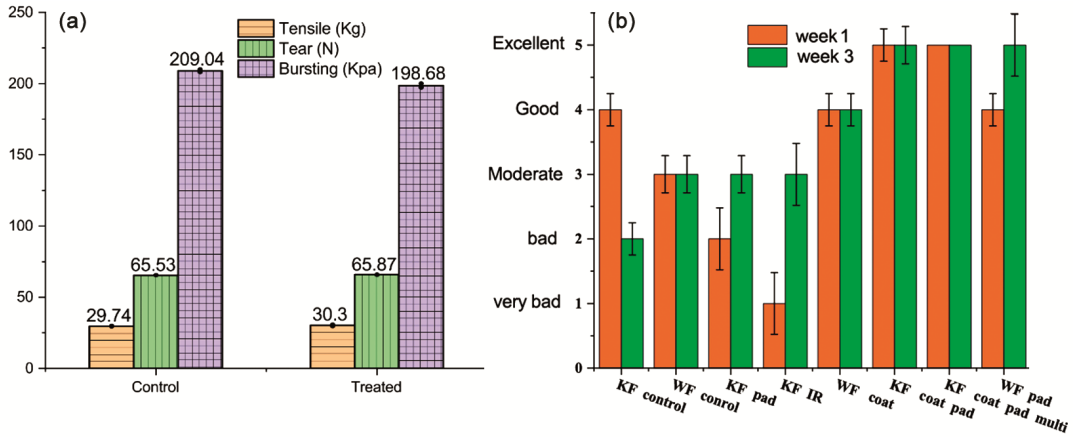

Fig. 6 — Comparative evaluation of untreated and treated fabric samples (a) mechanical properties, and (b) odour assessment

untreated knit fabric exhibits a bursting strength of 208 kPa, but this decreases to 198.68 kPa (standard error 1.4) in the treated sample, representing a 10.36 kPa decrease compared to the control sample. This decrease is attributed to the coating formulation used during treatment, which includes binders and other chemicals. While the polymeric coating enhances tensile and tear strength by providing structural reinforcement, it simultaneously increases the rigidity of the fabric. This added stiffness reduces elasticity, which is crucial for resisting multi-directional stresses, thereby lowering the bursting strength.

Although carbonised water hyacinth treatment does not significantly enhance the mechanical properties of fabrics, it has shown notable improvements when incorporated into composites. Films produced from alkali-treated water hyacinth via thermal compression demonstrate a tensile strength of 1.869 MPa and an elongation of 1.25%[28]. Additionally, reinforced with 6% NaOH-treated water hyacinth fibres, show substantial improvements in tensile, flexural, and impact strength compared with untreated counterparts[29].

3.5 Odour Test Analysis

The odour evaluation results are illustrated in Fig. 6 (b). The findings show that, except for the knit control sample (KF control), most untreated and treated fabrics develop noticeable odour during the first week. However, the odour intensity gradually reduces over time. Among the untreated samples, the woven fabric maintains a stable moderate odour level (standard error 0.25), whereas the untreated knit fabric exhibits a progressive increase in odour intensity. Among the treated samples, knit fabrics finished using the coated and IR methods demonstrate relatively weaker odour resistance. In contrast, the best performance is observed in knit fabrics treated using the coated followed by multiple padded applications (KF coat pad multi). These samples show complete odour resistance, producing no detectable odour in both week 1 and week 3 assessments, with a standard error of zero. This strong performance suggests that the coating–padding combination ensures effective and uniform deposition of carbonised water hyacinth particles, enabling efficient suppression of odour-causing microbial activity.

3.6 SEM and EDS

The SEM micrograph in Fig. 7 (a) shows the morphology of carbonised water hyacinth particles. The particles exhibit predominantly spherical to oval shapes, with an average length of 2.46 µm and a width of approximately 100 nm. The nanoparticles are not randomly dispersed; instead, they are preferentially located along the fibre surfaces and within the inter-fibre voids. A substantial portion is embedded between fibres, while others adhere to fibre surfaces through the binding agents employed during the coating process. The particles possess a distinctive curvature, resulting in a concave oval morphology.

These structural characteristics have important thermal implications. Carbon exhibits diverse thermal behaviour depending on its form. For instance, pyrolytic graphite possesses exceptionally high thermal conductivity—second only to type-II diamond—while conventional graphite displays much lower conductivity due to weak interlayer bonding[30]. Carbon nanoparticles also show variable thermal behaviour; for example, carbon nanotubes (CNTs) significantly enhance thermal conductivity when dispersed in poly-alpha-olefin (PAO) oils[31]. The SEM image reveals a 3D arrangement of carbon nanoparticles with a relatively uniform distribution

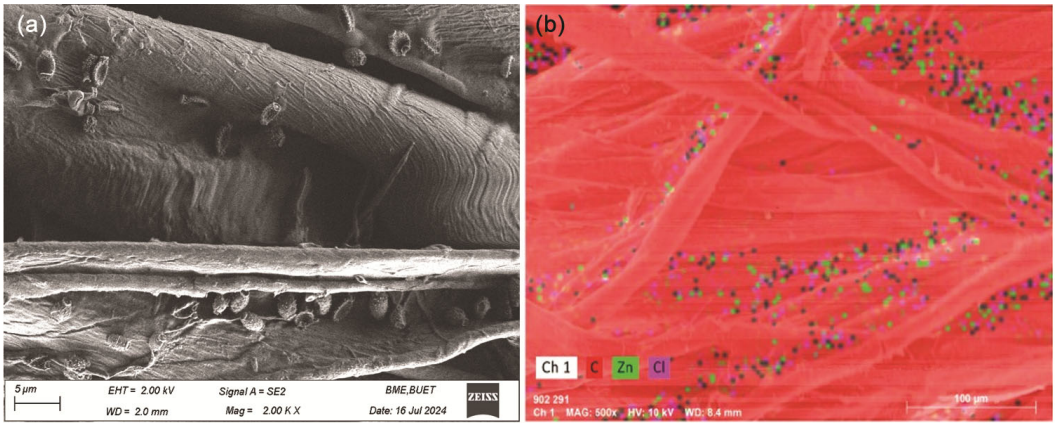

Fig. 7 — SEM and EDS of carbonised water hyacinth-treated samples (a) SEM image, and (b) EDS analysis

Table 3 — Elemental composition determined from EDS analysis

Element	At.no.	Mass norm, %	Atom, %	Abs. error, 3 sigma
C	6	99.32	99.87	9.46
Zn	30	0.68	0.68	0.13
Cl	17	0.00	0.00	0.00

along the Z-direction. This arrangement helps reduce heat loss perpendicular to the fabric plane, contributing to improved insulation[32]. The curved surface of carbonised water hyacinth particles further enhances insulation by creating micro-air pockets that trap heat. However, the particle dispersion is not entirely uniform. The presence of gaps and clustering, as visible in Fig. 8(a), limits the overall improvement in insulation to around 14%. Achieving a more homogeneous distribution may therefore further enhance thermal performance.

Fig. 7 (b) presents the EDS analysis of the treated samples. The spectra identify three elements: carbon (C), zinc (Zn), and chlorine (Cl). Notably, the carbon content is significantly higher than that of the other elements in Table 3. Carbon dominates the composition, with a mass-normalised percentage of 99.32%, confirming the extensive deposition of carbon nanoparticles. Zinc is present only in trace amounts (0.68%), originating from zinc chloride used during chemical activation. Chlorine appears at negligible levels and does not influence material properties. The strong carbon peak near 5 keV confirms its abundant presence, while the much smaller Zn and Cl peaks at 1 keV and 2.6 keV, respectively, confirm their minor contributions.

4 Conclusion

This study demonstrates that carbonised and chemically activated water hyacinth can serve as a functional finishing material for textiles. The carbonisation process produces concave oval-shaped carbon nanoparticles that successfully adhere to fabric surfaces through padding, coating, and combined application methods. Although the treatment does not substantially enhance mechanical properties such as tensile, tear, or bursting strength, it does not compromise fabric integrity and, in some cases, provides marginal reinforcement due to the polymeric coating. The treated fabrics show notable improvements in thermal behaviour, with increases of 13.8% in thermal insulation and 14.3% in thermal resistance, attributable to the unique morphology and distribution of carbon nanoparticles. The most significant functional enhancement is observed in odour resistance, where samples treated through coating followed by multiple padding exhibit complete odour suppression over repeated assessments. SEM and EDS analyses confirm successful deposition and high carbon content within the treated fabrics, with nanoparticles forming structured arrangements that contribute to thermal performance. The findings establish that activated carbon derived from water hyacinth—an abundant and invasive biomass—offers a sustainable, low-cost, and effective approach for developing odour-resistant and thermally enhanced textile materials. The future expansion of this research work is to incorporate the nanoparticles into commercial socks to make them odour-free.

Acknowledgement

The authors gratefully acknowledge Mr Md. Sumon Mia for his assistance with the thermal properties tests. We also thank the Centre for Research and Industrial Relations (CRIR) wing of the National Institute of Textile Engineering and Research, Dhaka, Bangladesh, for providing support in terms of machinery and raw materials.

References

1 Danish M & Ahmad T, *Renew Sustain Energy Rev*, 87 (2018) 1.
2 Carroll G T & Kirschman D L, *ACS Omega*, 7 (50) (2022) 46640.
3 Lozano-Castelló D, Cazorla-Amorós D, Linares-Solano A & Quinn D F, *Carbon*, 40 (15) 2817.
4 Cataldi P, Lamanna L, Bertei C, Arena F, Rossi P, Liu M, Fonzo D F, Papageorgiou D G, Luzio A & Caironi M, *Adv Funct Mater*, 32 (23) (2022) 2113417.
5 Anusorn B, *J Environ Viology*, 36 (1) (2015) 1143.
6 Mu'azu N, Jarrah N, Zubair M & Alagha O, *Int J Environ Res Public Health*, 14 (10) (2017) 1094.
7 Chen Y Y, Jiang W P, Chen H L, Huang H C, Huang G J, Chiang H M, Chang C C, Huang C L & Juang T Y, *RSC Adv*, 11 (27) (2021) 16661.
8 Tobias V D, Conrad J L, Mahardja B & Khanna S, *Biol Invasions*, 21 (12) (2019) 3479.
9 Lahon D, Sahariah D, Debnath J, Nath N, Meraj G, Farooq M, Kanga S, Singh S K & Chand K, *Peer J*, 11 (2023) 14811.
10 Barua V B, Goud V V & Kalamdhad A S, *Renew Energy*, 126 (2018) 21.
11 Sukasem N, Khanthi K & Prayoonkham S, *Energy Procedia*, 138 (2017) 294.
12 Rezania S, Ponraj M, Din M F M, Songip A R, Sairan F M & Chelliapan S, *Renew Sustain Energy Rev,* 41 (2015) 943.
13 Mohammad A H, Radovic I, Ivanović M & Kijevčanin M, *Sustainability*, 14 (18) (2022) 11144.
14 Gunasekaran G, Prakash C & Periyasamy S, *J Nat Fibers*, 18 (3) (2021) 355.
15 Leyden J J, McGinley K J, Hölzle E, Labows J N & Kligman A M, *J Invest Dermatol*, 77 (5) (1981) 413.

16 Xu Y, McQueen R & Wismer W, *J Text Appar Technol Manag*, 3 (2013) 8.
17 Teufel L, Schuster K C, Merschak P, Bechtold T & Redl B, *Microb Physiol*,14 (4) (2008) 193.
18 Rathinamoorthy R & Thilagavathi G J, *J Text Appar Technol Manag*, 9 (2014)
19 McQueen R H, Laing R M, Delahunty C M & Brooks H J L, *J Text Inst*, 99 (6) (2008) 515.
20 Huang J, *J Therm Biol*, 31 (6) (2006) 461.
21 Incropera F P, DeWitt D P, Bergman T L & Lavine A S, *Fundamentals of heat and mass transfer*, (Wiley, Hoboken, N J) (2007) 997.
22 Collet F & Pretot S, *Constr Build Mater*, 65 (2014) 612.
23 Abubakar M, Raji A & Hassan M A, *Niger J Technol*, 37 (1) (2018) 108.
24 Kono J, Goto Y, Ostermeyer Y, Frischknecht R & Wallbaum H, *Key Eng Mater*, 678 (2016) 1.
25 Peirce F T & Rees W H, *J Text Inst Trans*, 37 (1946) 181.
26 Parsons K C, *Ergonomics*, 991 (1988).
27 Salas-Ruiz A, Del Mar Barbero-Barrera M & Ruiz-Téllez T, *Materials*, 12 (4) (2019) 560.
28 Le D H, Phung M K H, Nguyen T T & Nguyen V V L, *Key Eng Mater*, 999 (2024) 81.
29 Owen M M, Achukwu E O & M d Akil H, *J Nat Fibers*, 19 (16) (2022) 13970.
30 Ruoff R S, Lorents D C, *Carbon*, 33 (7) (1995) 925.
31 Shaikh S, Lafdi K & Ponnappan R, *J Appl Phys*, (2007) 101064302.
32 Tang B, Wang Y, Hu L, Lin L, Ma C, Zhang C, Lu Y, Sun K & Wu X, *J Eng Fibers Fabr*, 14 (2019) 1.